

Article

Ground-State Tautomerism and Excited-State Proton Transfer in 7-Hydroxy-4-methyl-8-((phenylimino)methyl)-2H-chromen-2-one as a Potential Proton Crane

Daniela Nedeltcheva-Antonova ^{1,2}  and Liudmil Antonov ^{1,*} ¹ Institute of Electronics, Bulgarian Academy of Sciences, 1784 Sofia, Bulgaria; daniela.nedeltcheva@gmail.com² Institute of Organic Chemistry with Centre of Phytochemistry, Bulgarian Academy of Sciences, 1113 Sofia, Bulgaria

* Correspondence: liudmil.antonov@gmail.com

Abstract: The tautomerism in the title compound as a potential long-range proton transfer (PT) switch has been studied by using the DFT and TD-DFT approaches. The data show that in aprotic solvents, the enol tautomer dominates, while the increase in the content of the keto tautomer (short-range PT) rises as a function of polarity of the solvent. In ethanol, due to specific solute–solvent stabilization through intermolecular hydrogen bonding, a substantial amount of the keto forms exists in solution. The irradiation leads to two competitive processes in the excited state, namely ESIPT and trans/cis isomerization around the azomethine bond as in other structurally similar Schiff bases. The studied compound is not suitable for bistable tautomeric switching, where long-range PT occurs, due to the difficult enolization of the coumarin carbonyl group.

Keywords: 7-hydroxy-coumarin; 7-hydroxy-3-methylcoumarin; Schiff base; tautomerism; DFT; TD-DFT; solvent effect; molecular switching; proton crane; proton transfer



Citation: Nedeltcheva-Antonova, D.; Antonov, L. Ground-State Tautomerism and Excited-State Proton Transfer in 7-Hydroxy-4-methyl-8-((phenylimino)methyl)-2H-chromen-2-one as a Potential Proton Crane. *Physchem* **2024**, *4*, 91–105. <https://doi.org/10.3390/physchem4010007>

Academic Editors: Aggelos Avramopoulos and James A. Platts

Received: 11 December 2023

Revised: 10 January 2024

Accepted: 6 March 2024

Published: 11 March 2024



Copyright: © 2024 by the authors. Licensee MDPI, Basel, Switzerland. This article is an open access article distributed under the terms and conditions of the Creative Commons Attribution (CC BY) license (<https://creativecommons.org/licenses/by/4.0/>).

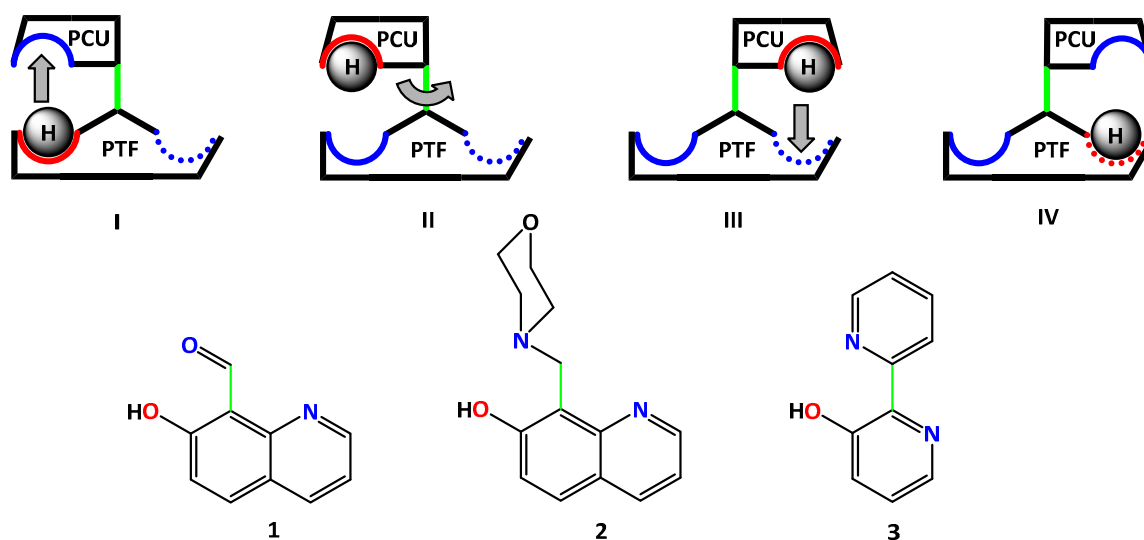
1. Introduction

Excited-state intramolecular proton transfer (ESIPT) is a feature of organic molecules, containing strong proton-donating/accepting groups, which, due to the increased acidity/basicity in the excited state, exchange a proton over the short distance of pre-existing hydrogen bonding [1–10]. ESIPT-exhibiting molecules have become a field of active research in recent decades, due to their applications as light-emitting materials and laser dyes [11–15], optical sensors [16–27], organic light-emitting diodes [20,21,28–36], optical storage devices [37] and photo stabilizers [38]. The same process underlies a special class of bistable photo switches [39], called proton cranes, where the ESIPT is accompanied by intramolecular rotation [40], leading to the transport of a movable proton from one side of the molecule to another.

The overall process of switching in proton cranes is outlined in Scheme 1. The proton, which is located at the proton donor site of a PT frame (PTF), undergoes ESIPT to the proton crane unit (PCU) upon irradiation. In this way, the proton is separated from the PTF, in which two free proton acceptor sites remain. The competition between them is the driving force of the rotation of the PCU, which can lead to the delivery and release of the proton to the other side of the PTF. The overall process can be classified as long-range intramolecular proton transfer.

Depending on the extent of conjugation between PTF and PCU, and more importantly, on the possibility for tautomeric proton exchange between PTF and PCU, the switching mechanism can be very different [41,42]. In **1** [43,44], the ESIPT (i.e., the transition from **I*** to **II***) leads to tautomeric structural re-arrangement, which changes the nature of the axle from a single to a double bond. This causes twisting around the axle to a structure where the PTF and PCU are perpendicular each other, and relaxation to the ground state occurs through

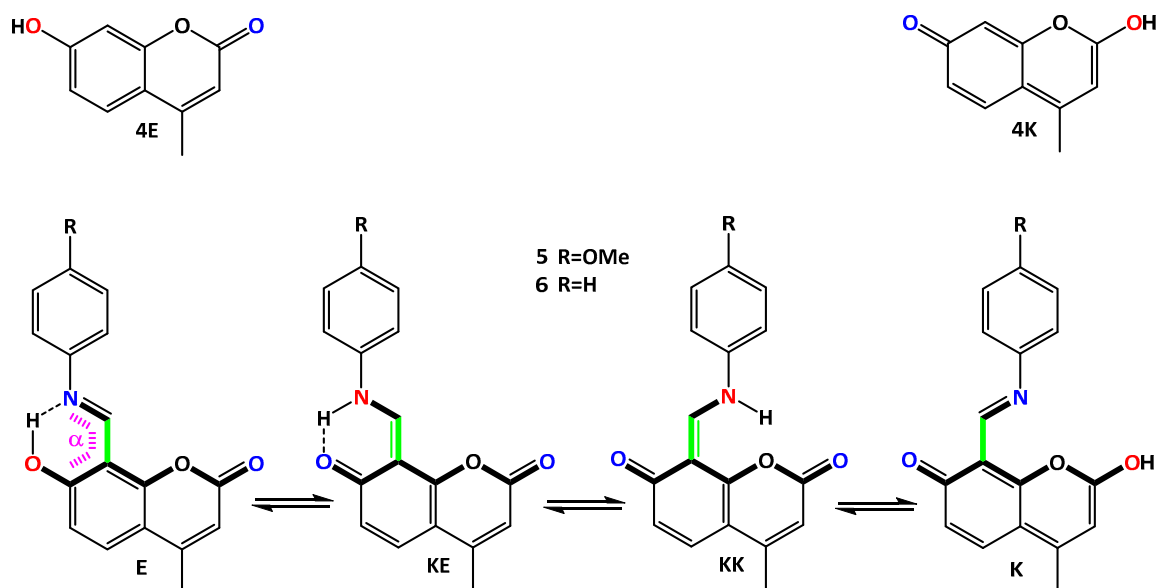
conical intersection. As a result, **II** and **III** are populated simultaneously, leading (at suitable relative energies) to a population of **I** and **IV**, respectively. In **2** [42,45–47], the initial ESIPT leads to **II***, which has a zwitterionic structure (i.e., intramolecular deprotonation occurs). The nature of the axle remains unchanged and the long-range PT occurs entirely in the excited state, which leads to **IV***, where the PTF is protonated again. Then, the relaxation to the ground state populates **IV**. In **3** [48–50], there is also possibility for tautomeric rearrangement in the first stage of the process, but due to the highly unstable zwitterionic nature of **IV**, the end state has never been reached [49,50].



Scheme 1. Sketch of a molecular switch, based on a long-range intramolecular PT. The red color indicates proton donor sites, while blue is used for proton acceptor sites. The twisting axle is shown in green. Below, three compounds, as experimentally studied examples, are shown.

7-hydroxy-quinoline is one of the most frequently studied examples for long-range intramolecular proton transfer [51–61] and is a very suitable structure for PTF, where the proton donor OH group and the proton acceptor N atom are far apart to provide conditions for truly intramolecular proton exchange. The enol tautomer is substantially more stable, while the NH tautomer has been experimentally observed only in protic organic solvents or in the presence of water and results from the intermolecular, solvent-assisted PT mechanism [43,61]. Previous computational studies suggested that the reversible long-range PT process could be observed for a series of 7-hydroxy-quinoline-based switches and oxazine [41,62] and other six-membered ring heterocycles [62], pyridines [62–64], the carbaldehyde group [43], and CO-BF₂ [65,66] as proton cranes units. Recently, we have reported several classes of proton cranes, where the azomethine group plays the role of a PCU, providing intramolecular PT to **III**, and in limited cases to **IV**, upon irradiation [67,68].

7-hydroxy-coumarin and its derivatives (including **4**, Scheme 2), also possess a proton donor group (O-H) at a large distance from the proton acceptor group (C=O), making direct intramolecular PT impossible. The substantially more stable enol form is observed in organic solvents, while the keto form appears in the presence of alcohols, water and organic bases as for 7-hydroxy-coumarin [69–74] as well as for **4** [74–79]. As reported for **4**, concentration-assisted PT takes place in the gas phase [80] as well. Quite interestingly, in 7-hydroxy-4-(trifluoromethyl)coumarin in toluene, the addition of 1-methylimidazole leads to excited-state intermolecular long-range PT in the picosecond time scale, where the base acts as a proton-transfer shuttle from the hydroxyl group to the carbonyl [81].



Scheme 2. Enol (4E) and keto (4K) tautomers of 7-hydroxy-4-methylcoumarin (**up**). Possible tautomeric forms and mechanism for intramolecular long-range PT in the Schiff bases, discussed in the current study (**down**). The skeleton important for the switching is given in bold lines. The twisting angle α is indicated in magenta.

In spite of its structural suitability as a PTF, 7-hydroxycoumarin and its derivative **4** have never been considered in the design of proton cranes. Very recently, the synthesis and spectral properties of **5** have been reported, along with some photochemical information [82,83]. This creates a solid background for detailed theoretical studies that can reveal the ground-state tautomeric properties and excited-state PT in **6** as simplified models of **5**. Bearing in mind that the Ph rings in the Schiff bases are partially out of planarity, the effect of weak substituents like OMe on the tautomeric state is negligible [84]. In the current investigation, the tautomerism of **6** in the ground and excited state is studied in a variety of solvents, and the applicability of 7-hydroxy-coumarin Schiff bases as proton cranes is considered.

2. Computational Details

Quantum-chemical calculations in the ground state were performed using the Gaussian 16 C.01 program suite [85]. All structures (in both the ground and excited state) were optimized without restrictions, using tight optimization criteria and an ultrafine grid in the computation of two-electron integrals and their derivatives. The true minima were verified by performing frequency calculations in the corresponding environment. The implicit solvation was described using the Polarizable Continuum Model [86] (the integral equation formalism variant, IEFPCM, as implemented in Gaussian 16). The transition states were estimated using the Berny algorithm [87] and again verified by performing frequency calculations in the corresponding environment.

The M06-2X [88,89] density functional with the TZVP [90] basis set was used for the structure optimizations in the ground state. This fitted hybrid meta-GGA functional with 54% HF exchange was especially developed to describe main-group thermochemistry and non-covalent interactions. The use of M06-2X provides very good predictability of the ground-state tautomerism [68,91,92] in tautomeric compounds and proton cranes in solution, as well as the E/Z isomerization ratio in rotary switches.

The TD-DFT method [93,94] was used for singlet excited-state optimizations. CAM-B3LYP [95] with the TZVP basis set was used for the optimizations (NStates = 6). The selection of CAM-B3LYP was based on its better performance (in comparison with a variety of density functionals, including M06-2X) in describing electronic excitation energies, excited-

state geometries, dipole moments and oscillator strengths in a variety of systems [96–99], including ESIPT ones [100], as well as from our own previous experience [68,101].

Bearing in mind that M06-2X systematically underestimates vertical transition energies [102], the UV-Vis spectral data were predicted by the B3LYP [103] functional (6-311 + G(2d,p) basis set) using the M06-2X optimized ground-state geometries. The corresponding spectral curves (presented as molar absorptivities) were constructed from the theoretically obtained band positions and oscillator strengths by using Gauss band shape [104] according to Equation (1) as follows:

$$\varepsilon(\lambda) = \sum_{i=1}^n \varepsilon_{max,i} \cdot e^{-\ln(2) \cdot 10^{14} \cdot \left(\frac{\frac{1}{\lambda_{max,i}} - \frac{1}{\lambda}}{\frac{\Delta\nu_{1/2}}{2}} \right)^2} \quad (1)$$

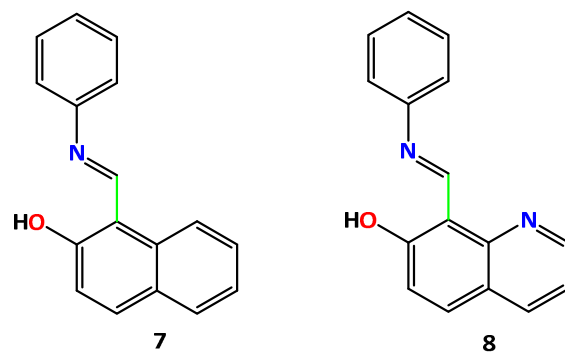
where n is the number of the transitions taken into account, $\lambda_{max,i}$ is the predicted position of the band of the i th transition in nm and $\varepsilon_{max,i}$ is the calculated maximal intensity of the i th band according to Equation (2) from the oscillator strength f_i [105].

$$\varepsilon_{max,i} = \frac{f_i}{7.04 \times 10^{-9} \cdot \Delta\nu_{1/2}} \quad (2)$$

A half-band width ($\Delta\nu_{1/2}$) value of 3500 cm^{-1} was used for all bands.

3. Results and Discussion

The possible tautomeric forms of **5** and **6** are given in Scheme 2. According to the data, obtained by Liubimov and co-authors [82], the **E** tautomer of **5**, absorbing in the near UV range (340 nm), is substantially more stable in aprotic solvents like toluene. The **KE** form has an absorption maximum around 450 nm, the intensity of which arises in protic solvents. The same behavior is typical for the tautomeric Schiff bases derived from 2-naphthol (**7**, Scheme 3) [84] and 7-hydroxy-quinoline (**8**) [68], which feature intramolecular hydrogen bonding and increased aromaticity in the OH-containing part.



Scheme 3. Schiff bases, possessing intramolecular hydrogen bonding.

The absorption spectra of the possible tautomers of **6**, as a model of **5**, are shown in Figure 1 and Figure S1 in toluene and acetonitrile, respectively. In line with the experiment, the **E** tautomer absorbs around 330–340 nm, which corresponds very well to the experimental data in these two solvents [82,83]. The existence of the keto tautomers (**KE**, **KK** and **K**) should be manifested by the appearance of red-shifted absorbance, each of them with their own signature. According to the relative stabilities of the tautomers, shown in Figure 2 and, in detail, in Table S1, the energy difference between **E** and **KE** suggests a very small amount of the latter is presented in toluene and acetonitrile, with more in the latter. The energies of **KK**, and especially of **K**, are too high to be observed in solution. According to the spectrum of **5** in toluene [82], a very low intensive tail is observed in the range 400–500 nm, while in acetonitrile [83], the red-shifted band is well defined at 450 nm, which corresponds to the suggested spectra of **KE** and **KK**. As discussed above, due to the high relative energy (>6 kcal/mol in respect of **E**, Table S1), the **KK** tautomer should be

excluded. In the case of **6**, the appearance of **KE** has an individual feature, which differs from the **E** to **KE** transitions in **7** and **8**. While in **7** and **8**, the increase in the content of the **KE** form leads to a decrease in the intensity of the band assigned to the enol [68,84], in the case of **6**, as very clearly seen from Figure 1 and Figure S1, the increase in the keto form should also lead to a rise in the absorption at 340 nm, due to the overlapping between the S_0-S_1 transition of **E** and the S_0-S_n transitions in **KE**, with the latter having larger oscillator strength. Actually, this is observed for **5**, comparing the molar absorptivities at 340 nm in toluene and ethanol [82]. The intensity of the band in toluene is $\sim 23\,000\text{ M}^{-1}\cdot\text{cm}^{-1}$, which nicely corresponds to that in Figure 1. The same value in ethanol, where the content of **KE** is substantially higher, is much larger. Based on the predicted theoretical data for the **KE** maximum in ethanol with molar absorptivity around $9\,000\text{ M}^{-1}\cdot\text{cm}^{-1}$ (Figure S2) and the measured value in ethanol ($4\,500\text{ M}^{-1}\cdot\text{cm}^{-1}$), it can be estimated roughly that the amount of **5KE** is between 40 and 50%. This is surprisingly high compared to the predicted relative energies in ethanol as a medium (Table 1), suggesting that this tautomeric state can be only attributed to a specific solute–solvent stabilization.

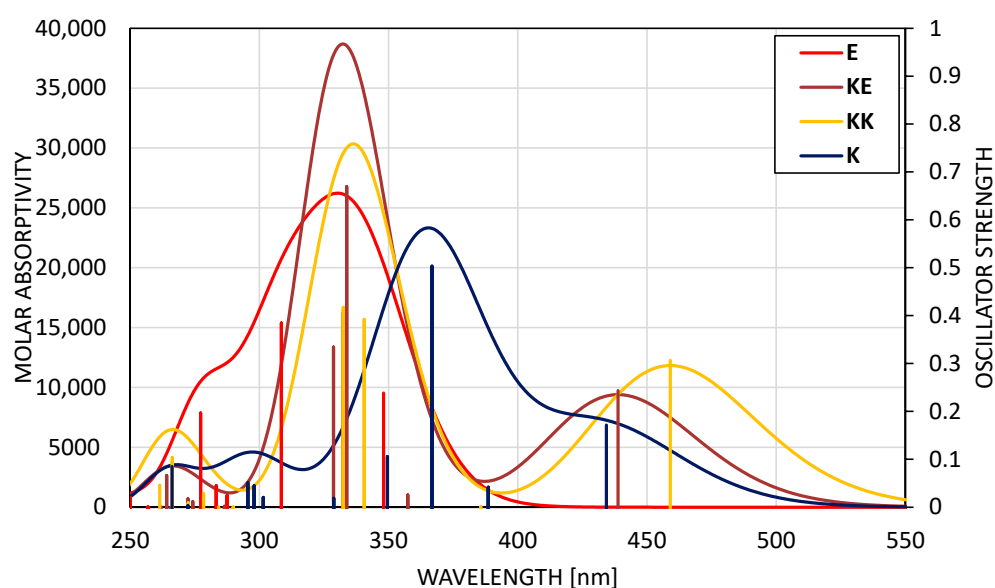


Figure 1. Predicted absorption spectra of the tautomers of **6** in toluene (in acetonitrile, see Figure S1).

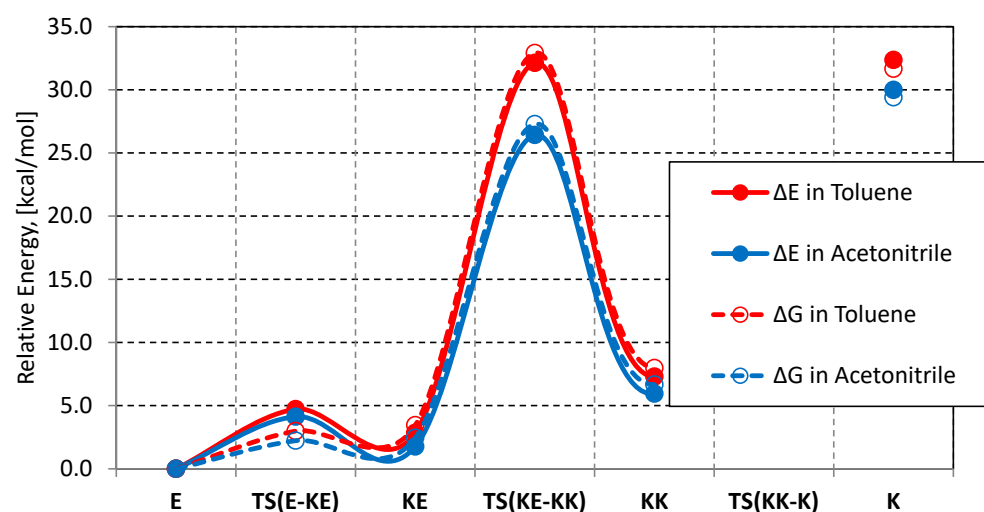
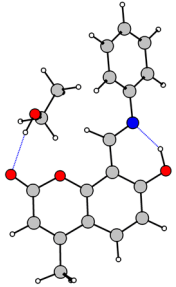
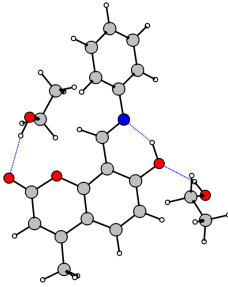
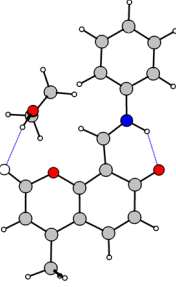
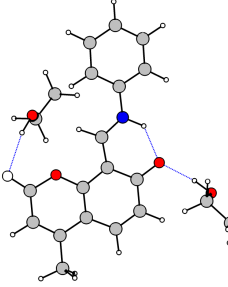
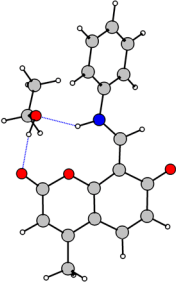
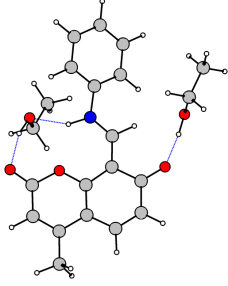
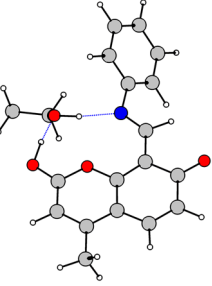


Figure 2. Potential energy surface of **6** in the ground state. DE is the relative total energy, while DG is the relative Gibbs free energy. Detailed information is provided in Table S1.

Table 1. Relative energies of the 1:1 and 1:2 complexes of **6** with ethanol molecules in the ethanol environment. The corresponding values for the single tautomers in the same environment are given in brackets.

Structure	Relative Energetics [kcal/mol] (M06-2X/TZVP)		Structure	Relative Energetics [kcal/mol] (M06-2X/TZVP)	
	ΔE	$\Delta\Delta G$		ΔE	$\Delta\Delta G$
 E + EtOH	0.0 (0.0)	0.0 (0.0)	 E + 2EtOH	1.34	0.24
 KE + EtOH	0.99 (1.80)	1.36 (2.50)	 KE + 2EtOH	0.0	0.0
 KK + EtOH	3.4 (6.0)	3.9 (6.8)	 KK + 2EtOH	0.93	2.63
 K + EtOH	17 (30)	15 (29)	K + 2EtOH	spontaneously goes to KK	

As seen from Table 1, the relative stability of the tautomers in ethanol (as implicit solvation) suggests around 5% of **KE**, which is much lower than the observed value. Even a very simple explicit solvation model with one molecule solvent attached changes the situation substantially. The relative stability of **KE** increases to almost 15%, which shows

the reasons for substantial stabilization in alcohols. The increase in the number of attached solvent molecules would probably shift the equilibrium further to the keto tautomer, as shown in the case of two ethanol molecules being attached, where the solvent stabilization of **KE** is substantial. Although the structure of the **KK** + EtOH and **K** + EtOH complexes, shown in Table 1, suggest that a channel for the exchange of the proton between **KK** and **K** potentially exists, the energy of the latter is too high to be really populated in solution. It is especially interesting to mention that this solvent channel actually works in the direction of the more stable **KK**, as seen from the 1:2 complex of **K**. Of course, the data, collected in Table 1, represent a very simplified model of the reality in solution, but they show the trends in the change in the tautomeric state as a result of the specific solvation.

The discussion up to now has been based on the theoretical simulations, which logically raises the concern of how reliable these conclusions are, especially because there are no quantitative data about the position of the tautomeric **E–KE** equilibrium in **5** and **6** to confirm the reliability of using the M06-2X/TZVP approach for the relative stability prediction. On one hand, it was previously proved that the M06-2X/TZVP level of theory predicts, in a reliable way, the tautomeric state and important structural characteristics of azodyes and Schiff bases in aprotic solvents [91]. On the other hand, experimental data are available for **7** and **8**, where the same theoretical approach was used [68]. The corresponding information to compare **6–8** is collected in Table 2.

Table 2. Theoretically predicted ΔE and ΔG values compared with the experimentally determined ΔG values at room temperature in toluene and acetonitrile (in brackets).

Structure	Relative Energetics [kcal/mol]							
	6		7			8		
	M06-2X/TZVP		M06-2X/TZVP		[84]	M06-2X/TZVP		[68]
	ΔE	ΔG	ΔE	ΔG	ΔG_{exp}	ΔE	ΔG	ΔG_{exp}
E	0.0 (0.0)	0.0 (0.0)	0.0 (0.0)	0.0 (0.0)	0.0 (0.0)	0.0 (0.37)	0.0 (0.10)	(0.52)
KE	2.8 (1.76)	3.5 (2.4)	1.70 (0.55)	1.80 (0.60)	1.42 * (0.35)	0.52 (0.0)	0.62 (0.0)	(0.0)
KK	7.3 (6.0)	8.0 (6.7)	9.0 (7.1)	9.8 (8.3)	-	1.9 (0.70)	2.05 (0.63)	- (1.0)
K	32 (30)	32 (29)	-	-	-	7.6 (4.8)	7.5 (4.7)	-

* in cyclohexane.

As seen from the data in Table 2, there is reasonable agreement between the theoretically obtained ΔE values and the experimental Gibbs free energies for **7** and **8**. Of course, as it was underlined above, this agreement is limited to aprotic solvents, since the implicit solvation model does not account the specific solute–solvent interactions with the protic solvents. This means, for instance, that the theoretical results for alcohols, obtained by using the PCM solvation only, have to be interpreted with care. The information given in Table 1 is a very convincing example.

The data collected in Table 2 allow to make conclusions about the effect of the PTF in compounds **6–8**. In all three compounds in toluene, the enol is the most stable form, but the relative stability of the **KE** form increases from **6** to **8**, from an almost negligible amount in **6** to almost 1/3 of the total population in **8**. The **KK** form is strongly destabilized in **7**, due to steric hindrance between the tautomeric NH and the C₈H proton, and in **6**, due to the lack of stabilizing hydrogen bonding as in **8**. The **K** tautomer does not exist in **7** and is very strongly destabilized in **6**. The latter is a result of the difficult enolization of the carbonyl group in the coumarin backbone and/or by the strong stabilization of the

enol form within the 7-hydroxy-coumarin core. In structurally similar compounds, where 7-hydroxy-coumarin plays a role of potential PTF, and where benzothiazole [106,107] and other conjugated nitrogen-containing heterocycles [22,108] are attached as PCU, there is no evidence of the existence of **KK** and **K** switched forms.

According to the data reported by Liubimov and co-authors [82], in toluene **5** exhibits a single emission band around 545 nm. The isolated PTU, **4**, also show a single band, but it is substantially blue shifted (at around 380 nm), which is attributed to the local emission of the only existing in this solvent enol tautomer. Therefore, the substantial Stokes shift ($11\,000\text{ cm}^{-1}$) in **5** suggests an ESIPT process from **E*** to **KK*** as the authors stated. Additional irradiation does not lead to spectral changes in **5** in in this solvent.

In Figure 3, the ground- and first excited-state potential energy surfaces are sketched. According to these, and also to the general understanding of long-range PT in similar compounds [41], the excitation of the enol form through an energetically high Franck–Condon state could lead either spontaneously to conical intersection (CI) relaxation in the C=N bond isomerization region, yielding a mixture of ground-state **E** and **Ecis**, or ballistically, through ESIPT, to **KE***. Then, the excited **KE*** can emit or, by twisting around the C-C bond (the axle in Scheme 2), can reach the twisting conical intersection region, relaxing as a mixture of **KE** and **KK**. As shown above, **KE** almost immediately restores to the predominant **E**, while **KK** can be accumulated due to the large relaxation barrier back ($\sim 25\text{ kcal/mol}$ in respect of **KK**). Only in such a consequence of events could an emission from **KK** be observed. Bearing in mind that no spectral changes are observed upon irradiation, the accumulation of **KK** is less probable to be assumed. Therefore, the observed red-shifted emission could be only attributed to **KE***. The large Stokes shift of this emission probably comes from the substantial stabilization of **KE*** in respect of the enolic Franck–Condon state, as seen from the figure. Schiff base **8** also exhibits an ESIPT emission in toluene around 490 nm with a Stokes shift of 7400 cm^{-1} [68], which comes from it being lower in energy, compared to here, in the Franck–Condon state. An emission in cyclohexane around 480 nm, attributed to the ESIPT process [109], is measured for **7**, but there are no theoretical data to make a more detailed interpretation.

The situation dramatically changes in both **4** and **5** going to an ethanol solution [82]. As seen from Figure 4, the emission spectrum of **6** depends on the excitation wavelength; a single emission band with a maximum at 530 nm is observed when excited at 461 nm (spectrum 3), whereas two emission bands with maxima at 442 nm and 530 nm are observed when excited at 375 nm (spectra 2 and 5). According to the discussion above, in the ground state, a substantial amount of **KE** exists in ethanol, expressed by the red-shifted band at around 450 nm. Therefore, the emission observed upon excitation at 461 nm can be attributed to the **KE*** as it is observed in toluene.

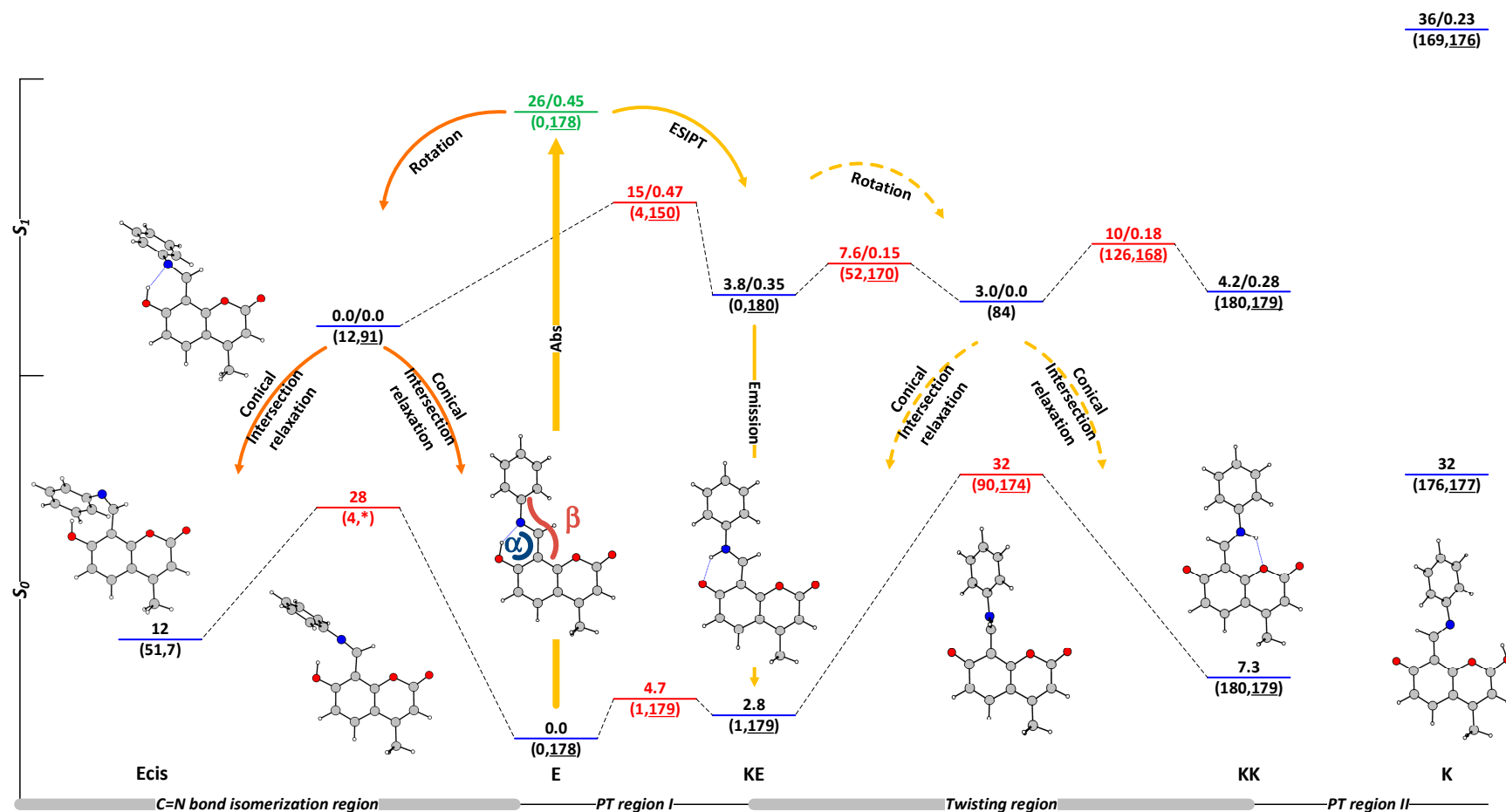


Figure 3. Ground-(M06-2X) and first excited-state (CAM-B3LYP) potential energy surface of 6 in toluene. The stable structures are indicated in blue; the transition states are indicated in red. The Franck–Condon state of the enol form is shown in green. The relative energies are given in kcal/mol units. In the excited states, the oscillator strength is listed after the energy, separated by a slash. The values of the angles α (describing the twisting motion around the axle, see Scheme 2) and β (describing the trans to cis isomerization of the azomethine bond) are given in brackets; the second one is underlined.

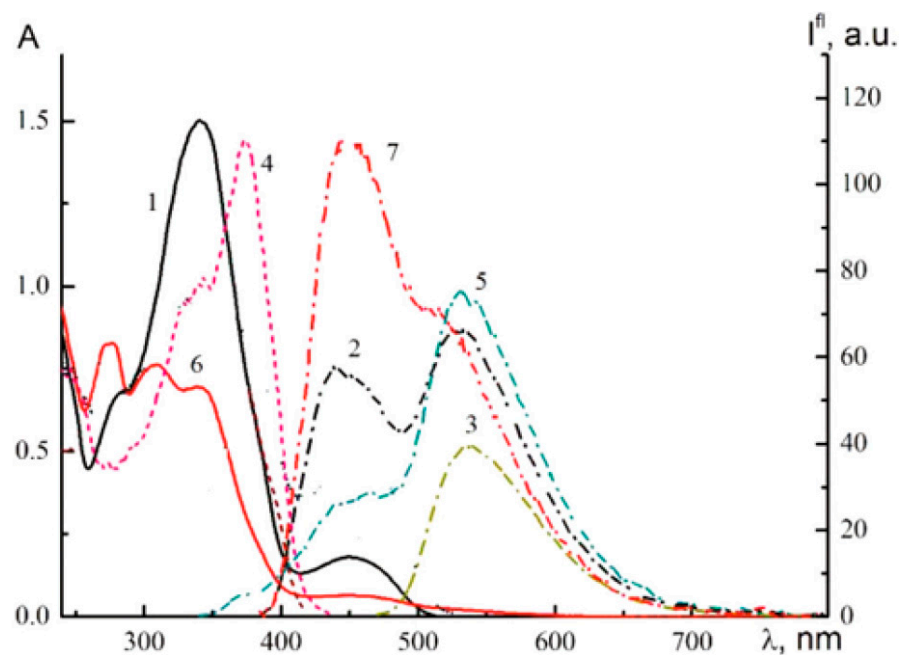


Figure 4. Absorption spectrum (1), fluorescence spectra at $\lambda_{\text{ex}} = 332$ (5), 375 nm (2, 7), and 461 nm (3), and fluorescence excitation spectrum at $\lambda_{\text{reg}} = 461$ nm (4) before (1–5) and after (6, 7) UV irradiation with the external source of high intensity of compound (4) in ethanol. Reproduced from [82] with permission from the Springer Nature BV.

Since, in the region around 380 nm, both **E** and **KE** are absorbing, the excitation in this region leads to an emission at 530 nm, attributed to the existing **KE**, and to an emission at 442 nm (missing in toluene), which probably comes from the enol form, where the tautomeric OH group is engaged in intermolecular hydrogen bonding with the solvent. From the existing data, it is impossible to make a conclusion as to whether the intramolecular O-H...N bonding is completely or partially broken by the solvent. As seen from Figure 4, upon irradiation with an external light source, substantial spectral changes are observed, associated with a rise in the emission at 440 nm. Basically, the irradiation can lead to two processes, as shown in Figure 3—trans/cis isomerization to **Ecis** or switching—leading to the accumulation of **KK**. The latter process should be more probable in toluene, where switching relaxation back from **KK** to **KE** through **TS(KE-KK)** is expected to be slower. The ground-state twisting transition state is very polar, and its energy decreases from 32 kcal/mol in toluene (Table S1) to 26 kcal/mol in ethanol, considered as an implicit solvent. The real stabilization is probably higher because of the increased possibilities for specific solute–solvent interactions in the transition state, in which the NH proton does not participate in intramolecular hydrogen bonding. It is much more probable to assume trans to cis isomerization with the accumulation of some amounts of **Ecis**. This form (as seen from Figure S2) is blue shifted compared to **E**, and the intramolecular hydrogen bonding is broken, which allows additional stabilization by the solvent. The relaxation back to **E** proceeds through the inversion transition state (as predicted by the theoretical calculations, Figure 3), in which energy does not depend on the solvent polarity. The process of cis/trans isomerization has been already described in structural analogues of **6** by Traven and co-authors [110,111]. A very recent study by Tang and co-workers describes the breakage of the CO-O bond in alcohols under strong external irradiation [112] in **4**. The same process is theoretically predicted by Krauter et al [71], which creates an additional possibility in the interpretation of the data from Figure 4.

4. Conclusions

The tautomerism of 7-hydroxy-4-methyl-8-((phenylimino)methyl)-2H-chromen-2-one has been studied by using the density functional theory in ground and excited states, and

the theoretical data were considered in comparison with the existing experimental results. Although the studied compound can potentially exist as a mixture of four tautomers, the enol form dominates in the ground state in aprotic solvents. Small amounts of the short-range proton-transferred keto tautomer are observed as a function of the polarity of the solvent. In ethanol, the content of the keto tautomer is substantial as a result of its specific stabilization by the solvent. According to the theoretical data, the long-range PT could not be observed due to the difficulty of the enolization of the carbonyl group in the coumarin frame. Upon excitation, two competitive processes could be expected, namely ESIPT and trans to cis isomerization, around the azomethine bond. However, the existing experimental data and their theoretical interpretation suggest that the latter is much more probable.

Supplementary Materials: The following supporting information can be downloaded at: <https://www.mdpi.com/article/10.3390/physchem4010007/s1>, Figure S1: Predicted absorption spectra of the tautomers of **6** in acetonitrile; Figure S2: Predicted absorption spectra of the tautomers and isomers of **6** in ethanol; Table S1: Relative energies of the tautomers of **6** and their spectral parameters in toluene and in acetonitrile (in brackets) in the ground state.

Author Contributions: Conceptualization, L.A.; methodology, L.A. and D.N.-A.; investigation, L.A. and D.N.-A.; resources, L.A.; writing—original draft preparation, L.A.; writing—review and editing, L.A. and D.N.-A.; visualization, L.A.; supervision, L.A.; project administration, L.A.; funding acquisition, L.A. All authors have read and agreed to the published version of the manuscript.

Funding: The author thanks the Bulgarian National Science Fund, National Research Program VIHREN, by the project T-Motors (contracted as KP-06-DV-9/2019) for the financial support for this investigation. We also acknowledge the provided access to the e-infrastructure of the NCHDC B—part of the Bulgarian National Roadmap on RIs—with the financial support of Grant No. D01-168/2022.

Data Availability Statement: Data is contained within the article or Supplementary Materials.

Conflicts of Interest: The authors declare no conflict of interest.

References

1. Weller, A. Über die Fluoreszenz der Salizylsäure und verwandter Verbindungen. *Naturwissenschaften* **1955**, *42*, 175–176. [CrossRef]
2. Weller, A. Innermolekularer Protonenübergang Im Angeregten Zustand. *Z. Elektrochem. Berichte Bunsenges. Phys. Chem.* **1956**, *60*, 1144–1147. [CrossRef]
3. Arnaut, L.G.; Formosinho, S.J. Excited-State Proton Transfer Reactions I. Fundamentals and Intermolecular Reactions. *J. Photochem. Photobiol. A Chem.* **1993**, *75*, 1–20. [CrossRef]
4. Formosinho, S.J.; Arnaut, L.G. Excited-State Proton Transfer Reactions II. Intramolecular Reactions. *J. Photochem. Photobiol. A Chem.* **1993**, *75*, 21–48. [CrossRef]
5. Hynes, J.T.; Klinman, J.P.; Limbach, H.-H.; Schowen, R.L. (Eds.) *Hydrogen-Transfer Reactions*; Wiley-VCH: Weinheim, Germany, 2006; ISBN 978-3-527-61154-6.
6. Demchenko, A.P.; Tang, K.-C.; Chou, P.-T. Excited-State Proton Coupled Charge Transfer Modulated by Molecular Structure and Media Polarization. *Chem. Soc. Rev.* **2013**, *42*, 1379–1408. [CrossRef]
7. Antonov, L. (Ed.) *Tautomerism: Methods and Theories*; Wiley-VCH: Weinheim, Germany, 2014; ISBN 978-3-527-33294-6.
8. Serdiuk, I.E.; Roshal, A.D. Exploring Double Proton Transfer: A Review on Photochemical Features of Compounds with Two Proton-Transfer Sites. *Dye. Pigment.* **2017**, *138*, 223–244. [CrossRef]
9. Joshi, H.C.; Antonov, L. Excited-State Intramolecular Proton Transfer: A Short Introductory Review. *Molecules* **2021**, *26*, 1475. [CrossRef] [PubMed]
10. Jankowska, J.; Sobolewski, A.L. Modern Theoretical Approaches to Modeling the Excited-State Intramolecular Proton Transfer: An Overview. *Molecules* **2021**, *26*, 5140. [CrossRef] [PubMed]
11. Kwon, J.E.; Park, S.Y. Advanced Organic Optoelectronic Materials: Harnessing Excited-State Intramolecular Proton Transfer (ESIPT) Process. *Adv. Mater.* **2011**, *23*, 3615–3642. [CrossRef] [PubMed]
12. Tsutsui, M.; Taniguchi, M. Single Molecule Electronics and Devices. *Sensors* **2012**, *12*, 7259–7298. [CrossRef] [PubMed]
13. Sakai, K.; Tsuzuki, T.; Itoh, Y.; Ichikawa, M.; Taniguchi, Y. Using Proton-Transfer Laser Dyes for Organic Laser Diodes. *Appl. Phys. Lett.* **2005**, *86*, 081103. [CrossRef]
14. Chen, K.-Y.; Hsieh, C.-C.; Cheng, Y.-M.; Lai, C.-H.; Chou, P.-T. Extensive Spectral Tuning of the Proton Transfer Emission from 550 to 675 nm via a Rational Derivatization of 10-Hydroxybenzo[h]quinoline. *Chem. Commun.* **2006**, 4395. [CrossRef]
15. Stoerkler, T.; Pariat, T.; Laurent, A.D.; Jacquemin, D.; Ulrich, G.; Massue, J. Excited-State Intramolecular Proton Transfer Dyes with Dual-State Emission Properties: Concept, Examples and Applications. *Molecules* **2022**, *27*, 2443. [CrossRef]

16. Sedgwick, A.C.; Wu, L.; Han, H.-H.; Bull, S.D.; He, X.-P.; James, T.D.; Sessler, J.L.; Tang, B.Z.; Tian, H.; Yoon, J. Excited-State Intramolecular Proton-Transfer (ESIPT) Based Fluorescence Sensors and Imaging Agents. *Chem. Soc. Rev.* **2018**, *47*, 8842–8880. [[CrossRef](#)]
17. Li, Y.; Dahal, D.; Abeywickrama, C.S.; Pang, Y. Progress in Tuning Emission of the Excited-State Intramolecular Proton Transfer (ESIPT)-Based Fluorescent Probes. *ACS Omega* **2021**, *6*, 6547–6553. [[CrossRef](#)]
18. Chen, L.; Fu, P.; Wang, H.; Pan, M. Excited-State Intramolecular Proton Transfer (ESIPT) for Optical Sensing in Solid State. *Adv. Opt. Mater.* **2021**, *9*, 2001952. [[CrossRef](#)]
19. Shekhovtsov, N.A.; Bushuev, M.B. Enol or Keto? Interplay between Solvents and Substituents as a Factor Controlling ESIPT. *J. Mol. Liq.* **2022**, *361*, 119611. [[CrossRef](#)]
20. Shekhovtsov, N.A.; Nikolaenkova, E.B.; Ryadun, A.A.; Vorobyeva, S.N.; Krivopalov, V.P.; Bushuev, M.B. Dual Emission of ESIPT-Capable 2-(2-Hydroxyphenyl)-4-(1 *H*-Pyrazol-1-Yl)Pyrimidines: Interplay of Fluorescence and Phosphorescence. *New J. Chem.* **2023**, *47*, 6361–6377. [[CrossRef](#)]
21. Shekhovtsov, N.A.; Ryadun, A.A.; Bushuev, M.B. Luminescence of a Zinc(II) Complex with a Protonated 1-Hydroxy-1 *H*-imidazole ESIPT Ligand: Direct Excitation of a Tautomeric Form. *ChemistrySelect* **2021**, *6*, 12346–12350. [[CrossRef](#)]
22. Nikolaeva, O.G.; Popova, O.S.; Dubonosova, I.V.; Karlutova, O.Y.; Dubonosov, A.D.; Bren, V.A.; Minkin, V.I. Spectral-Luminescent and Ionochromic Properties of Azomethine Imine-Coumarin Conjugates. *Russ. J. Gen. Chem.* **2022**, *92*, 841–849. [[CrossRef](#)]
23. Minkin, V.I.; Tsukanov, A.V.; Dubonosov, A.D.; Bren, V.A. Tautomeric Schiff Bases: Iono-, Solvato-, Thermo- and Photochromism. *J. Mol. Struct.* **2011**, *998*, 179–191. [[CrossRef](#)]
24. Wang, D.; Li, S.-J.; Cao, W.; Wang, Z.; Ma, Y. ESIPT-Active 8-Hydroxyquinoline-Based Fluorescence Sensor for Zn(II) Detection and Aggregation-Induced Emission of the Zn(II) Complex. *ACS Omega* **2022**, *7*, 18017–18026. [[CrossRef](#)] [[PubMed](#)]
25. Bren, V.A.; Dubonosov, A.D.; Popova, O.S.; Revinskii, Y.V.; Tikhomirova, K.S.; Minkin, V.I. Synthesis and Photo- and Ionochromic and Spectral-Luminescent Properties of 5-Phenylpyrazolidin-3-One Azomethine Imines. *Int. J. Photoenergy* **2018**, *2018*, 9746534. [[CrossRef](#)]
26. Bren, V.A.; Popova, O.S.; Tolpygin, I.E.; Chernoiyanov, V.A.; Revinskii, Y.V.; Dubonosov, A.D. New Ionochromic Azomethinimine Chemosensors. *Russ. Chem. Bull.* **2015**, *64*, 668–671. [[CrossRef](#)]
27. Popova, O.S.; Bren, V.A.; Tkachev, V.V.; Utenyshev, A.N.; Revinskii, Y.V.; Tikhomirova, K.S.; Starikov, A.G.; Borodkin, G.S.; Dubonosov, A.D.; Shilov, G.V.; et al. Benzenoid-Quinoid Tautomerism of Azomethines and Their Structural Analogs 56. Azomethine Imines, Derivatives of Salicylic and 2-Hydroxynaphthoic Aldehydes. *Russ. Chem. Bull.* **2016**, *65*, 648–653. [[CrossRef](#)]
28. Shekhovtsov, N.A.; Vorob'eva, S.; Nikolaenkova, E.B.; Ryadun, A.A.; Krivopalov, V.P.; Gourlaouen, C.; Bushuev, M.B. Complexes on the Base of a Proton Transfer Capable Pyrimidine Derivative: How Protonation and Deprotonation Switch Emission Mechanisms. *Inorg. Chem.* **2023**, *62*, 16734–16751. [[CrossRef](#)]
29. Fu, P.-Y.; Yi, S.-Z.; Pan, M.; Su, C.-Y. Excited-State Intramolecular Proton Transfer (ESIPT) Based Metal–Organic Supramolecular Optical Materials: Energy Transfer Mechanism and Luminescence Regulation Strategy. *Acc. Mater. Res.* **2023**, *4*, 939–952. [[CrossRef](#)]
30. Shekhovtsov, N.A.; Ryadun, A.A.; Plyusnin, V.F.; Nikolaenkova, E.B.; Tikhonov, A.Y.; Bushuev, M.B. First 1-Hydroxy-1 *H*-Imidazole-Based ESIPT Emitter with an O–H ··· O Intramolecular Hydrogen Bond: ESIPT-Triggered TICT and Speciation in Solution. *New J. Chem.* **2022**, *46*, 22804–22817. [[CrossRef](#)]
31. Shekhovtsov, N.A.; Nikolaenkova, E.B.; Berezin, A.S.; Plyusnin, V.F.; Vinogradova, K.A.; Naumov, D.Y.; Pervukhina, N.V.; Tikhonov, A.Y.; Bushuev, M.B. Tuning ESIPT-Coupled Luminescence by Expanding π -Conjugation of a Proton Acceptor Moiety in ESIPT-Capable Zinc(II) Complexes with 1-Hydroxy-1 *H*-Imidazole-Based Ligands. *Dalton Trans.* **2022**, *51*, 15166–15188. [[CrossRef](#)]
32. Trannoy, V.; Léaustic, A.; Gadan, S.; Guillot, R.; Allain, C.; Clavier, G.; Mazerat, S.; Geffroy, B.; Yu, P. A Highly Efficient Solution and Solid State ESIPT Fluorophore and Its OLED Application. *New J. Chem.* **2021**, *45*, 3014–3021. [[CrossRef](#)]
33. Shekhovtsov, N.A.; Nikolaenkova, E.B.; Berezin, A.S.; Plyusnin, V.F.; Vinogradova, K.A.; Naumov, D.Y.; Pervukhina, N.V.; Tikhonov, A.Y.; Bushuev, M.B. A 1-Hydroxy-1 *H*-imidazole ESIPT Emitter Demonstrating anti-Kasha Fluorescence and Direct Excitation of a Tautomeric Form. *ChemPlusChem* **2021**, *86*, 1436–1441. [[CrossRef](#)]
34. Petdee, S.; Chaiwai, C.; Benchaphanthawee, W.; Nalaoh, P.; Kungwan, N.; Namuangruk, S.; Sudyoosuk, T.; Promarak, V. Imidazole-Based Solid-State Fluorophores with Combined ESIPT and AIE Features as Self-Absorption-Free Non-Doped Emitters for Electroluminescent Devices. *Dye. Pigment.* **2021**, *193*, 109488. [[CrossRef](#)]
35. Long, Y.; Mamada, M.; Li, C.; Dos Santos, P.L.; Colella, M.; Danos, A.; Adachi, C.; Monkman, A. Excited State Dynamics of Thermally Activated Delayed Fluorescence from an Excited State Intramolecular Proton Transfer System. *J. Phys. Chem. Lett.* **2020**, *11*, 3305–3312. [[CrossRef](#)] [[PubMed](#)]
36. Shekhovtsov, N.A.; Nikolaenkova, E.B.; Ryadun, A.A.; Samsonenko, D.G.; Tikhonov, A.Y.; Bushuev, M.B. ESIPT-Capable 4-(2-Hydroxyphenyl)-2-(Pyridin-2-Yl)-1H-Imidazoles with Single and Double Proton Transfer: Synthesis, Selective Reduction of the Imidazolic OH Group and Luminescence. *Molecules* **2023**, *28*, 1793. [[CrossRef](#)] [[PubMed](#)]
37. Park, S.; Kim, S.; Seo, J.; Park, S.Y. Application of Excited-State Intramolecular Proton Transfer (ESIPT) Principle to Functional Polymeric Materials. *Macromol. Res.* **2008**, *16*, 385–395. [[CrossRef](#)]
38. Smith, T.P.; Zaklika, K.A.; Thakur, K.; Walker, G.C.; Tominaga, K.; Barbara, P.F. Ultrafast Studies on Proton Transfer in Photostabilizers. *J. Photochem. Photobiol. A Chem.* **1992**, *65*, 165–175. [[CrossRef](#)]
39. Feringa, B.L.; Browne, W.R. (Eds.) *Molecular Switches*, 2nd ed.; Wiley-VCH: Weinheim, Germany, 2011; ISBN 978-3-527-63440-8.

40. Nedeltcheva-Antonova, D.; Antonov, L. Controlled Tautomerism: Is It Possible? In *Tautomerism: Concepts and Applications in Science and Technology*; Antonov, L., Ed.; Wiley-VCH: Weinheim, Germany, 2016; pp. 273–294. ISBN 978-3-527-69571-3.
41. Sobolewski, A.L. Reversible Molecular Switch Driven by Excited-State Hydrogen Transfer. *Phys. Chem. Chem. Phys.* **2008**, *10*, 1243–1247. [[CrossRef](#)]
42. van der Loop, T.H.; Ruesink, F.; Amirjalayer, S.; Sanders, H.J.; Buma, W.J.; Woutersen, S. Unraveling the Mechanism of a Reversible Photoactivated Molecular Proton Crane. *J. Phys. Chem. B* **2014**, *118*, 12965–12971. [[CrossRef](#)]
43. Vetokhina, V.; Nowacki, J.; Pietrzak, M.; Rode, M.F.; Sobolewski, A.L.; Waluk, J.; Herbich, J. 7-Hydroxyquinoline-8-Carbaldehydes. 1. Ground- and Excited-State Long-Range Prototropic Tautomerization. *J. Phys. Chem. A* **2013**, *117*, 9127–9146. [[CrossRef](#)]
44. Lapinski, L.; Rostkowska, H.; Nowacki, J.; Nowak, M.J. Photoinduced Long-Distance Hydrogen-Atom Transfer in Molecules with a 7-Hydroxyquinoline Frame and a Carbaldehyde or Aldoxime Group as the Intramolecular Hydrogen Transporting Crane. *J. Phys. Chem. A* **2023**, *127*, 3104–3113. [[CrossRef](#)]
45. de Bekker, E.J.A.; Geerlings, J.D.; Varma, C.A.G.O. Mechanism of a Photoinduced Solvent-Assisted Transfer of a Proton to a Specified Remote Target. *J. Phys. Chem. A* **2000**, *104*, 5916–5927. [[CrossRef](#)]
46. Jalink, C.J.; Huizer, A.H.; Varma, C.A.G.O. Rotational Brownian Motion of the Proton Crane Operating in a Photoinduced Long-Distance Intramolecular Proton Transfer. *J. Chem. Soc. Faraday Trans.* **1992**, *88*, 1643. [[CrossRef](#)]
47. Jalink, C.J.; Huizer, A.H.; Varma, C.A.G.O. Rate-Limiting Action of a Proton Crane in Long-Range Intramolecular Proton Transfer. *J. Chem. Soc. Faraday Trans.* **1992**, *88*, 2655–2659. [[CrossRef](#)]
48. Kaczmarek, L.S. Bipyridines. Part XVIII. On the Synthesis of [2,2'-Bipyridine]-3-Ol and Other Novel 2,2'-Bipyridine Derivatives from [2,2'-Bipyridine]-3,3'-Diamine. *Bull. Pol. Acad. Sci. Tech. Sci.* **1985**, *33*, 401–409.
49. Kaczmarek, L.; Balicki, R.; Lipkowski, J.; Borowicz, P.; Grabowska, A. Structure and Photophysics of Deazabipyridyls. Excited Internally Hydrogen-Bonded Systems with One Proton Transfer Reaction Site. *J. Chem. Soc. Perkin Trans. 2* **1994**, 1603. [[CrossRef](#)]
50. Borowicz, P.; Grabowska, A.; Leś, A.; Kaczmarek, L.; Zagrodzki, B. New Phototautomerizing Systems: Non-Symmetric Derivatives of [2,2'-Bipyridyl]-3,3'-Diol. *Chem. Phys. Lett.* **1998**, *291*, 351–359. [[CrossRef](#)]
51. Ewing, G.W.; Steck, E.A. Absorption Spectra of Heterocyclic Compounds. I. Quinolinols and Isoquinolinols. *J. Am. Chem. Soc.* **1946**, *68*, 2181–2187. [[CrossRef](#)]
52. Mason, S.F. The Tautomerism of N-Heteroaromatic Hydroxy-Compounds. Part I. Infrared Spectra. *J. Chem. Soc.* **1957**, 4874–4880. [[CrossRef](#)]
53. Mason, S.F. The Tautomerism of N-Heteroaromatic Hydroxy-Compounds. Part II. Ultraviolet Spectra. *J. Chem. Soc.* **1957**, 5010–5017. [[CrossRef](#)]
54. Mason, S.F.; Philp, J.; Smith, B.E. Prototropic Equilibria of Electronically Excited Molecules. Part II. 3-, 6-, and 7-Hydroxyquinoline. *J. Chem. Soc. A* **1968**, 3051–3056. [[CrossRef](#)]
55. Lee, S.-I.; Jang, D.-J. Proton Transfers of Aqueous 7-Hydroxyquinoline in the First Excited Singlet, Lowest Triplet, and Ground States. *J. Phys. Chem.* **1995**, *99*, 7537–7541. [[CrossRef](#)]
56. García-Ochoa, I.; Bisht, P.B.; Sánchez, F.; Martínez-Atáz, E.; Santos, L.; Tripathi, H.B.; Douhal, A. Experimental and Theoretical Studies of the Proton-Hopping Reaction of 7-Hydroxyquinoline in Viscous Hydroxylic Media. *J. Phys. Chem. A* **1998**, *102*, 8871–8880. [[CrossRef](#)]
57. Chou, P.-T.; Wei, C.-Y.; Chris Wang, C.-R.; Hung, F.-T.; Chang, C.-P. Proton-Transfer Tautomerism of 7-Hydroxyquinolines Mediated by Hydrogen-Bonded Complexes. *J. Phys. Chem. A* **1999**, *103*, 1939–1949. [[CrossRef](#)]
58. Kwon, O.-H.; Lee, Y.-S.; Yoo, B.K.; Jang, D.-J. Excited-State Triple Proton Transfer of 7-Hydroxyquinoline along a Hydrogen-Bonded Alcohol Chain: Vibrationally Assisted Proton Tunneling. *Angew. Chem. Int. Ed.* **2006**, *45*, 415–419. [[CrossRef](#)] [[PubMed](#)]
59. Park, S.-Y.; Lee, Y.-S.; Kwon, O.-H.; Jang, D.-J. Proton Transport of Water in Acid–Base Reactions of 7-Hydroxyquinoline. *Chem. Commun.* **2009**, 926. [[CrossRef](#)]
60. Park, S.-Y.; Jang, D.-J. Excited-State Hydrogen Relay along a Blended-Alcohol Chain as a Model System of a Proton Wire: Deuterium Effect on the Reaction Dynamics. *Phys. Chem. Chem. Phys.* **2012**, *14*, 8885. [[CrossRef](#)]
61. Kumpulainen, T.; Lang, B.; Rosspointner, A.; Vauthey, E. Ultrafast Elementary Photochemical Processes of Organic Molecules in Liquid Solution. *Chem. Rev.* **2017**, *117*, 10826–10939. [[CrossRef](#)] [[PubMed](#)]
62. Rode, M.F.; Sobolewski, A.L. Effect of Chemical Substituents on the Energetical Landscape of a Molecular Photoswitch: An Ab Initio Study. *J. Phys. Chem. A* **2010**, *114*, 11879–11889. [[CrossRef](#)]
63. Benesch, C.; Rode, M.F.; Čížek, M.; Rubio-Pons, O.; Thoss, M.; Sobolewski, A.L. Switching the Conductance of a Single Molecule by Photoinduced Hydrogen Transfer. *J. Phys. Chem. C* **2009**, *113*, 10315–10318. [[CrossRef](#)]
64. Georgiev, A.; Antonov, L. 8-(Pyridin-2-Yl)Quinolin-7-Ol as a Platform for Conjugated Proton Cranes: A DFT Structural Design. *Micromachines* **2020**, *11*, 901. [[CrossRef](#)]
65. Csehi, A.; Illés, L.; Halász, G.J.; Vibók, Á. The Effect of Chemical Substituents on the Functionality of a Molecular Switch System: A Theoretical Study of Several Quinoline Compounds. *Phys. Chem. Chem. Phys.* **2013**, *15*, 18048–18054. [[CrossRef](#)]
66. Csehi, A.; Halász, G.J.; Vibók, Á. Molecular Switch Properties of 7-Hydroxyquinoline Compounds. *Int. J. Quantum Chem.* **2014**, *114*, 1135–1145. [[CrossRef](#)]
67. Nakashima, K.; Petek, A.; Hori, Y.; Georgiev, A.; Hirashima, S.; Matsushima, Y.; Yordanov, D.; Miura, T.; Antonov, L. Acylhydrazones Subunits as a Proton Cargo Delivery System in 7-Hydroxyquinoline. *Chem. Eur. J.* **2021**, *27*, 11559–11566. [[CrossRef](#)] [[PubMed](#)]

68. Georgiev, A.; Yordanov, D.; Ivanova, N.; Deneva, V.; Vassilev, N.; Kamounah, F.S.; Pittelkow, M.; Crochet, A.; Fromm, K.M.; Antonov, L. 7-OH Quinoline Schiff Bases: Are They the Long Awaited Tautomeric Bistable Switches? *Dye. Pigment.* **2021**, *195*, 109739. [[CrossRef](#)]
69. Grzywacz, J.; Taszner, S.; Kruszewski, J. Further Study on the Forms of Umbelliferone in Excited State. *Z. Naturforschung A* **1978**, *33*, 1307–1311. [[CrossRef](#)]
70. Taszner, S.; Grzywacz, J. Further Study on the Forms of Umbelliferone in Excited State. Part II. *Z. Naturforschung A* **1979**, *34*, 548–550. [[CrossRef](#)]
71. Krauter, C.M.; Möhring, J.; Buckup, T.; Pernpointner, M.; Motzkus, M. Ultrafast Branching in the Excited State of Coumarin and Umbelliferone. *Phys. Chem. Chem. Phys.* **2013**, *15*, 17846. [[CrossRef](#)]
72. Jacquemin, D.; Perpète, E.A.; Scalmani, G.; Frisch, M.J.; Assfeld, X.; Ciofini, I.; Adamo, C. Time-Dependent Density Functional Theory Investigation of the Absorption, Fluorescence, and Phosphorescence Spectra of Solvated Coumarins. *J. Chem. Phys.* **2006**, *125*, 164324. [[CrossRef](#)]
73. Sakurai, T.; Mizoguchi, H.; Yamada, S.; Inoue, H. Proton-Transfer Reactions between 7-Hydroxycoumarin and Tertiary Amines. Formation of the Ground-State Tautomer Anion. *Ber. Bunsenges. Phys. Chem.* **1996**, *100*, 505–507. [[CrossRef](#)]
74. Moriya, T. Excited-State Reactions of Coumarins in Aqueous Solutions. I. The Phototautomerization of 7-Hydroxycoumarin and Its Derivative. *Bull. Chem. Soc. Jpn.* **1983**, *56*, 6–14. [[CrossRef](#)]
75. Georgieva, I.; Trendafilova, N.; Aquino, A.; Lischka, H. Excited State Properties of 7-Hydroxy-4-Methylcoumarin in the Gas Phase and in Solution. A Theoretical Study. *J. Phys. Chem. A* **2005**, *109*, 11860–11869. [[CrossRef](#)] [[PubMed](#)]
76. Georgieva, I.; Trendafilova, N.; Aquino, A.J.A.; Lischka, H. Excited-State Proton Transfer in 7-Hydroxy-4-Methylcoumarin along a Hydrogen-Bonded Water Wire. *J. Phys. Chem. A* **2007**, *111*, 127–135. [[CrossRef](#)] [[PubMed](#)]
77. De Silva, N.; Minezawa, N.; Gordon, M.S. Excited-State Hydrogen Atom Transfer Reaction in Solvated 7-Hydroxy-4-Methylcoumarin. *J. Phys. Chem. B* **2013**, *117*, 15386–15394. [[CrossRef](#)]
78. Abdel-Mottaleb, M.S.A.; El-Sayed, B.A.; Abo-Aly, M.M.; El-Kady, M.Y. Fluorescence-Properties and Excited State Interactions of 7-Hydroxy-4-Methylcoumarin Laser Dye. *J. Photochem. Photobiol. A Chem.* **1989**, *46*, 379–390. [[CrossRef](#)]
79. Schulman, S.G.; Rosenberg, L.S. Tautomerization Kinetics of 7-Hydroxy-4-Methylcoumarin in the Lowest Excited Singlet State. *J. Phys. Chem.* **1979**, *83*, 447–451. [[CrossRef](#)]
80. Stamm, A.; Schwing, K.; Gerhards, M. Investigation of the Hydrated 7-Hydroxy-4-Methylcoumarin Dimer by Combined IR/UV Spectroscopy. *J. Chem. Phys.* **2014**, *141*, 194304. [[CrossRef](#)] [[PubMed](#)]
81. Westlake, B.C.; Paul, J.J.; Bettis, S.E.; Hampton, S.D.; Mehl, B.P.; Meyer, T.J.; Papanikolas, J.M. Base-Induced Phototautomerization in 7-Hydroxy-4-(Trifluoromethyl)Coumarin. *J. Phys. Chem. B* **2012**, *116*, 14886–14891. [[CrossRef](#)]
82. Liubimov, A.V.; Venidiktova, O.V.; Valova, T.M.; Shienok, A.I.; Koltsova, L.S.; Liubimova, G.V.; Popov, L.D.; Zaichenko, N.L.; Barachevsky, V.A. Photochromic and Luminescence Properties of a Hybrid Compound Based on Indoline Spiropyran of the Coumarin Type and Azomethinocoumarin. *Photochem. Photobiol. Sci.* **2018**, *17*, 1365–1375. [[CrossRef](#)]
83. Zaichenko, N.L.; Valova, T.M.; Venidiktova, O.V.; Lyubimov, A.V.; Shienok, A.I.; Koltsova, L.S.; Ayt, A.O.; Lyubimova, G.V.; Popov, L.D.; Barachevsky, V.A. Excited State Proton Transfers in Hybrid Compound Based on Indoline Spiropyran of the Coumarin Type and Azomethinocoumarin in the Presence of Metal Ions. *Molecules* **2021**, *26*, 6894. [[CrossRef](#)]
84. Antonov, L.; Fabian, W.M.F.; Nedeltcheva, D.; Kamounah, F.S. Tautomerism of 2-Hydroxynaphthaldehyde Schiff Bases. *J. Chem. Soc. Perkin Trans. 2* **2000**, 1173–1179. [[CrossRef](#)]
85. Frisch, M.J.; Trucks, G.W.; Schlegel, H.B.; Scuseria, G.E.; Robb, M.A.; Cheeseman, J.R.; Scalmani, G.; Barone, V.; Petersson, G.A.; Nakatsuji, H.; et al. *Gaussian 16 Rev. C.01*, Gaussian, Inc.: Wallingford, CT, USA, 2019.
86. Tomasi, J.; Mennucci, B.; Cammi, R. Quantum Mechanical Continuum Solvation Models. *Chem. Rev.* **2005**, *105*, 2999–3094. [[CrossRef](#)] [[PubMed](#)]
87. Schlegel, H.B. Optimization of Equilibrium Geometries and Transition Structures. *J. Comput. Chem.* **1982**, *3*, 214–218. [[CrossRef](#)]
88. Zhao, Y.; Truhlar, D.G. Density Functionals with Broad Applicability in Chemistry. *Acc. Chem. Res.* **2008**, *41*, 157–167. [[CrossRef](#)]
89. Zhao, Y.; Truhlar, D.G. The M06 Suite of Density Functionals for Main Group Thermochemistry, Thermochemical Kinetics, Noncovalent Interactions, Excited States, and Transition Elements: Two New Functionals and Systematic Testing of Four M06-Class Functionals and 12 Other Functionals. *Theor. Chem. Acc.* **2008**, *120*, 215–241. [[CrossRef](#)]
90. Schäfer, A.; Huber, C.; Ahlrichs, R. Fully Optimized Contracted Gaussian Basis Sets of Triple Zeta Valence Quality for Atoms Li to Kr. *J. Chem. Phys.* **1994**, *100*, 5829–5835. [[CrossRef](#)]
91. Antonov, L. Tautomerism in Azo and Azomethyne Dyes: When and If Theory Meets Experiment. *Molecules* **2019**, *24*, 2252. [[CrossRef](#)] [[PubMed](#)]
92. Rayne, S.; Forest, K. A Comparative Examination of Density Functional Performance against the ISOL24/11 Isomerization Energy Benchmark. *Comput. Theor. Chem.* **2016**, *1090*, 147–152. [[CrossRef](#)]
93. Improta, R. UV-Visible Absorption and Emission Energies in Condensed Phase by PCM/TD-DFT Methods. In *Computational Strategies for Spectroscopy*; Barone, V., Ed.; John Wiley & Sons, Inc.: Hoboken, NJ, USA, 2011; pp. 37–75. ISBN 978-1-118-00872-0.
94. Adamo, C.; Jacquemin, D. The Calculations of Excited-State Properties with Time-Dependent Density Functional Theory. *Chem. Soc. Rev.* **2013**, *42*, 845–856. [[CrossRef](#)]
95. Yanai, T.; Tew, D.P.; Handy, N.C. A New Hybrid Exchange–Correlation Functional Using the Coulomb-Attenuating Method (CAM-B3LYP). *Chem. Phys. Lett.* **2004**, *393*, 51–57. [[CrossRef](#)]

96. Li, R.; Zheng, J.; Truhlar, D.G. Density Functional Approximations for Charge Transfer Excitations with Intermediate Spatial Overlap. *Phys. Chem. Chem. Phys.* **2010**, *12*, 12697. [[CrossRef](#)]
97. Wang, J.; Durbeej, B. How Accurate Are TD-DFT Excited-state Geometries Compared to DFT Ground-state Geometries? *J. Comput. Chem.* **2020**, *41*, 1718–1729. [[CrossRef](#)]
98. Mahato, B.; Panda, A.N. Assessing the Performance of DFT Functionals for Excited-State Properties of Pyridine-Thiophene Oligomers. *J. Phys. Chem. A* **2021**, *125*, 115–125. [[CrossRef](#)] [[PubMed](#)]
99. Sarkar, R.; Boggio-Pasqua, M.; Loos, P.-F.; Jacquemin, D. Benchmarking TD-DFT and Wave Function Methods for Oscillator Strengths and Excited-State Dipole Moments. *J. Chem. Theory Comput.* **2021**, *17*, 1117–1132. [[CrossRef](#)]
100. Louant, O.; Champagne, B.; Liégeois, V. Investigation of the Electronic Excited-State Equilibrium Geometries of Three Molecules Undergoing ESIPT: A RI-CC2 and TDDFT Study. *J. Phys. Chem. A* **2018**, *122*, 972–984. [[CrossRef](#)]
101. Rode, M.F.; Nedeltcheva-Antonova, D.; Antonov, L. Long-Range Proton Transfer in 7-Hydroxy-Quinoline-Based Azomethine Dyes: A Hidden Reason for the Low Efficiency. *Molecules* **2022**, *27*, 8225. [[CrossRef](#)] [[PubMed](#)]
102. Antonov, L.; Kawachi, S.; Okuno, Y. Prediction of the Color of Dyes by Using Time-Dependent Density Functional Theory. *Bulg. Chem. Commun.* **2014**, *46*, 228–237.
103. Becke, A.D. Density-functional Thermochemistry. III. The Role of Exact Exchange. *J. Chem. Phys.* **1993**, *98*, 5648–5652. [[CrossRef](#)]
104. Antonov, L. Drawbacks of the Present Standards for Processing Absorption Spectra Recorded Linearly as a Function of Wavelength. *TrAC Trends Anal. Chem.* **1997**, *16*, 536–543. [[CrossRef](#)]
105. Antonov, L. (Ed.) Absorption UV-Vis Spectroscopy and Chemometrics: From Qualitative Conclusions to Quantitative Analysis. In *Tautomerism: Methods and Theories*; Wiley-VCH: Weinheim, Germany, 2013; pp. 25–47. ISBN 978-3-527-65882-4.
106. Xie, L.; Chen, Y.; Wu, W.; Guo, H.; Zhao, J.; Yu, X. Fluorescent Coumarin Derivatives with Large Stokes Shift, Dual Emission and Solid State Luminescent Properties: An Experimental and Theoretical Study. *Dye. Pigment.* **2012**, *92*, 1361–1369. [[CrossRef](#)]
107. Miksa, B. Fluorescent Dyes Used in Polymer Carriers as Imaging Agents in Anticancer Therapy. *Med. Chem.* **2016**, *6*, 611–639. [[CrossRef](#)]
108. Karcz, D.; Starzak, K.; Ciszkowicz, E.; Lecka-Szlachta, K.; Kamiński, D.; Creaven, B.; Jenkins, H.; Radomski, P.; Miłoś, A.; Ślusarczyk, L.; et al. Novel Coumarin-Thiadiazole Hybrids and Their Cu(II) and Zn(II) Complexes as Potential Antimicrobial Agents and Acetylcholinesterase Inhibitors. *Int. J. Mol. Sci.* **2021**, *22*, 9709. [[CrossRef](#)] [[PubMed](#)]
109. Joshi, H.; Kamounah, F.S.; Gooijer, C.; van der Zwan, G.; Antonov, L. Excited State Intramolecular Proton Transfer in Some Tautomeric Azo Dyes and Schiff Bases Containing an Intramolecular Hydrogen Bond. *J. Photochem. Photobiol. A Chem.* **2002**, *152*, 183–191. [[CrossRef](#)]
110. Traven, V.F.; Miroshnikov, V.S.; Pavlov, A.S.; Ivanov, I.V.; Panov, A.V.; Chibisova, T.A. Unusual E/Z-Isomerization of 7-Hydroxy-4-Methyl-8-[(9H-Fluoren-2-Ylimino)Methyl]-2H-1-Benzopyran-2-One in Acetonitrile. *Mendeleev Commun.* **2007**, *17*, 88–89. [[CrossRef](#)]
111. Traven, V.F.; Ivanov, I.V.; Panov, A.V.; Safronova, O.B.; Chibisova, T.A. Solvent-Induced E/Z(C=N)-Isomerization of Imines of Some Hydroxy-Substituted Formylcoumarins. *Russ. Chem. Bull.* **2008**, *57*, 1989–1995. [[CrossRef](#)]
112. Tang, Q.; Xian, Z.; Li, L.; Cao, H.; Wang, L.; Zheng, X. Study on the Photochemical Reaction Process of 4-Methyl-7-Hydroxycoumarin and Its Mechanism by Multi-Spectroscopic Technologies. *J. Phys. Conf. Ser.* **2021**, *2112*, 012023. [[CrossRef](#)]

Disclaimer/Publisher's Note: The statements, opinions and data contained in all publications are solely those of the individual author(s) and contributor(s) and not of MDPI and/or the editor(s). MDPI and/or the editor(s) disclaim responsibility for any injury to people or property resulting from any ideas, methods, instructions or products referred to in the content.